The van der Waals Complex between Boron Trifluoride and Methyl Fluoride: An Infrared and ab Initio Study

B. J. van der Veken* and E. J. Sluyts

Department of Chemistry, Universitair Centrum Antwerpen, Groenenborgerlaan 171, B 2020 Antwerp, Belgium

Received: June 25, 1997; In Final Form: September 3, 1997[⊗]

Mixtures of CH_3F and BF_3 have been investigated, using infrared spectroscopy, at low temperatures in the gas phase (170−210 K) and in solution in liquid argon (85−110 K) and in liquid krypton (115−165 K). In all cases, the formation of a 1:1 complex $CH_3F{\cdot}BF_3$ was observed. The complexation enthalpy was measured to be −16.8(5) kJ mol^{-1} in liquid argon and −18.0(3) kJ mol^{-1} in liquid krypton. Structural, energetic, and spectroscopic properties of the complex were calculated using ab initio methods at the MP2/6-31+G** level and are compared with the experimental data.

1. Introduction

Boron trifluoride is one of the most common catalysts in Friedel−Crafts alkylation reactions.[1] From early on, the catalytic action was attributed to a specific interaction between the Lewis base and the alkyl halide used. Such an interaction was originally demonstrated by Oláh et al.[2] These authors observed the formation of solid alkyl fluoride/boron trifluoride complexes when simple liquefied alkyl fluorides were saturated with BF_3 at temperatures between −50 and −100 °C. Melting and decomposition points of these complexes were determined, but apart from their stoichiometry, no structural or spectroscopic characteristics were reported. Recently, this phenomenon has triggered new studies. For instance, the simplest model for the complex is that formed between BF_3 and HF, and this complex has been studied using microwave spectroscopy and ab initio calculations.[3] Also, the formation of more realistic model complexes, using alkyl fluorides as Lewis bases, has been described using semiempirical[4] and ab initio calculations,[5] and in a preliminary report on a microwave analysis of the complex between CH_3F and BF_3, the van der Waals bond length has been reported.[6] Altogether, it is clear that detailed experimental studies on most aspects of these complexes are still lacking. Therefore, we have undertaken an infrared study of mixtures of BF_3 and CH_3F. The mixtures were investigated at low temperature in the gas phase and in cryosolution using liquid argon and krypton as solvents. In all phases, the formation of a complex was observed. In the following paragraphs we will report on the vibrational spectra, the stoichiometry, and the complexation enthalpy of the complex, and the results will be interpreted using ab initio calculations of structure, stability, and vibrational frequencies.

2. Experimental Section

Boron trifluoride was obtained from Union Carbide (CP grade), and methyl fluoride was purchased from PCR Inc. The solvent gases, argon and krypton, were supplied by L'Air Liquide and have purities of 99.9999% and 99.995%, respectively. In the vapor phase spectrum of the CH_3F used, no impurities could be detected. A small amount of SiF_4 was present in the BF_3 used; the krypton gas contained a very small amount of CF_4 as impurity.

The spectra were recorded on a Bruker model IFS 113v or on a Bruker 66v Fourier transform spectrometer, equipped with a globar source. In the mid-infrared region, a Ge/KBr beam splitter and a LN_2-cooled broad band MCT detector were used; in the far-infrared region, a 6 μm Mylar beam splitter and a LHe-cooled bolometer were used. For spectra in cryosolution, 200 scans were recorded at 0.5 cm^{-1} resolution, averaged, Happ Genzel apodized, and Fourier transformed with a zero-filling factor of 4. For the spectra of the gas-phase mixtures of BF_3 and CH_3F, the resolution was set at 0.25 cm^{-1}.

The liquid noble gas cell consists of the actual cell and a pressure manifold. The latter is used to fill and evacuate the cell and to monitor the amount of solute gases in each experiment. The cell has a path length of 4 cm and is equipped with wedged silicon windows. The procedure for preparing the solutions has been described before.[7] The gas-phase spectra were recorded in the same cell.

The spectra of solid CH_3F were obtained by depositing the compound on a CsI window, cooled to 10 K using a Leybold Heraeus ROK 10−300 cooling system. The same spectral conditions as for the cryosolutions were used.

The ab initio calculations were carried out using the Gaussian 94 software package[8] at the MP2/6-31+G** level. For all calculations the Berny optimization was used with the tight convergence option, and the correlation energy was calculated using all molecular orbitals. The vibrational spectra were calculated using the analytical (BF_3, CH_3F) or numerical ($CH_3F{\cdot}BF_3$) second derivatives from the analytically determined first derivatives of the energy with respect to the Cartesian coordinates.

3. Results

3.1. Ab Initio Calculations. Because previous theoretical studies on $BF_3{\cdot}CH_3F$ have not always discussed aspects of importance for a spectroscopic study, we have performed structural ab initio calculations at the MP2/6-31+G** level. The converged structure, together with essential geometrical data, is given in Figure 1. In agreement with the 3-21G structure described by Arnau et al.,[5] a van der Waals bond is formed between the fluorine atom of CH_3F and the electron deficient boron atom. The C−F bond makes an angle of approximately 120° with the B−F(C) van der Waals bond, leading to a complex with C_s symmetry. The van der Waals bond length obtained in this study, 2.3216 Å, compares favorably with the experimental[6] (C)F−B distance in $CH_3F{\cdot}BF_3$, 2.42 Å, but is much longer than the distance of 1.70 Å calculated by Arnau et al.[5] The serious underestimation of this distance in the latter study

[⊗] Abstract published in *Advance ACS Abstracts,* November 1, 1997.

S1089-5639(97)02078-1 CCC: $14.00

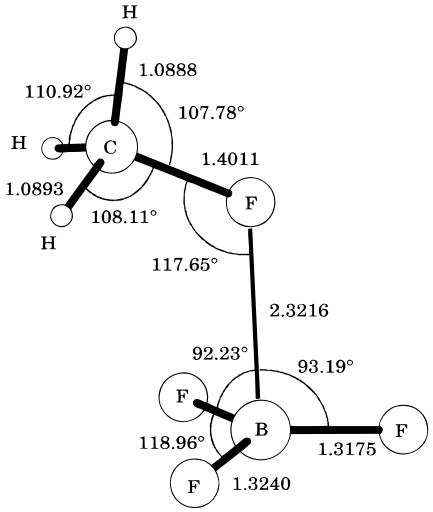

Figure 1. The ab initio structure, calculated at the MP2/6-31G** level, of the $CH_3F{\cdot}BF_3$ complex. Bond lengths are in angstroms, bond angles in degrees.

must be blamed on the limited basis set 3-21G. The in-plane C−H bond in the 3-21G structure is cis to the B−F(C) bond, while in our structure it is trans. The barrier toward rotation of the methyl group around the C−F bond is calculated to be 1.00 kJ mol^{-1}, while the barrier hindering the rotation of the methyl fluoride around the B−F(C) bond is only 0.7 kJ mol^{-1}. These values show that the complex is highly nonrigid, and it will be seen below that this is confirmed spectroscopically. The ab initio vibrational frequencies and infrared intensities of the monomers and of the complex, calculated in the harmonic approximation, and approximate descriptions of the modes involved are collected in Table 1. Comparison of the data reveals several interesting shifts, which will be discussed in relation to experiment below.

Finally, the complexation energy, defined as the energy of the complex from which the monomer energies have been subtracted, is −25.97 kJ mol^{-1}.

3.2. Gas-Phase Spectra. The ab initio complexation energy for $BF_3{\cdot}CH_3F$ suggests the complex is relatively stable. Thus, at temperatures at which vapor-phase spectra of the compounds can be usefully studied in a short path length cell, a measurable fraction of complex should be present. This is confirmed by the spectra shown in Figures 2 and 3, which were recorded from a mixture of CH_3F and BF_3, with an excess of the latter. In Figure 2, the region of the very intense CF stretch of CH_3F is given for a mixture recorded at 205 K. In this region, BF_3 shows no absorption bands, and the Q branch at 1047 cm^{-1}, with rotational fine structure in P and R branches, is the CF stretch in monomer CH_3F. The broad band on the low-frequency side of the monomer band, at 989 cm^{-1}, is assigned to the CF stretch of the complex. In a bond dipole model,[9] the dipole gradient for a characteristic vibration such as the CF stretch must be parallel to the bond in which the stretch is located. In the complex, the C−F bond shows a small angle with the *b* axis of the principal axis system, and hence, a predominant B type band is expected for this vibration. However, the band at 989 cm^{-1} shows no rotational structure. Using the ab initio rotational constants of the complex, 0.15512, 0.07388, and 0.07225 cm^{-1}, the pure type rigid rotor contours have been calculated[9] at 205 K. The B contour shows a PQ-QR structure with a QQ splitting of 2.0 cm^{-1}. Because of the strong overlap of the Q branches with the P and R branches, the latter show no separate maxima. The gas-phase contour of the BF_3 symmetric stretch, (ν_8), to be discussed in a next paragraph, shows substantial broadening.

TABLE 1: MP2/6-31+G Frequencies[a] and Infrared Intensities[b] of BF_3, CH_3F, and $CH_3F{\cdot}BF_3$**

species		assignment	$^{10}BF_3$	$^{11}BF_3$
A_1'	ν_1	BF sym stretch	873.5 (0)	873.5 (0)
A_2''	ν_2	BF out-of-plane def.	727.6 (127)	699.0 (118)
E'	ν_3	BF antisym stretch	1498.4 (1049)	1445.3 (967)
	ν_4	BF antisym def.	474.3 (30)[c]	472.4 (30)[c]

species		assignment	CH_3F
A_1	ν_1	CH sym stretch	3146.5 (33)
	ν_2	CH sym def.	1528.2 (5)
	ν_3	CF stretch	1059.4 (111)
E	ν_4	CH antisym stretch	3263.7 (53)[c]
	ν_5	CH antisym def	1553.9 (6.5)[c]
	ν_6	CH rocking	1216.5 (2.8)[c]

			$CH_3F{\cdot}BF_3$	
species		assignment	$^{10}BF_3$	$^{11}BF_3$
A′	ν_1	CH antisym stretch	3290.6 (13)	3290.5 (13)
	ν_2	CH sym stretch	3162.4 (24)	3162.4 (24)
	ν_3	CH antisym def.	1552.5 (9)	1552.4 (7)
	ν_4	CH sym def.	1523.7 (36)	1522.5 (8)
	ν_5	BF antisym stretch	1490.3 (447)	1438.2 (440)
	ν_6	CH rocking	1216.1 (2)	1216.1 (2)
	ν_7	CF stretch	1024.8 (104)	1024.4 (106)
	ν_8	BF sym stretch	859.8 (8)	859.6 (7)
	ν_9	BF out-of-plane def.	655.7 (258)	631.8 (236)
	ν_{10}	BF sym def.	477.0 (12)	475.1 (12)
	ν_{11}	F−B···F bend	187.4 (16)	187.2 (16)
	ν_{12}	B···F stretch	122.7 (15)	122.4 (15)
	ν_{13}	B···F−C bend	90.1 (1)	90.0 (1)
A″	ν_{14}	CH antisym stretch	3288.4 (10)	3288.4 (10)
	ν_{15}	CH antisym def.	1549.5 (1)	1549.2 (2)
	ν_{16}	BF antisym stretch	1460.9 (471)	1409.1 (434)
	ν_{17}	CF rocking	1212.9 (2)	1212.9 (2)
	ν_{18}	BF antisym def.	473.7 (12)	471.8 (12)
	ν_{19}	F−B···F antisym bend	170.1 (1)	170.0 (1)
	ν_{20}	H−C−F···B torsion	61.9 (1)	61.9 (1)
	ν_{21}	C−F···B−F torsion	32.6 (6)	32.6 (6)

[a] Frequencies in cm^{-1}. [b] Intensities in km mol^{-1} are indicated in parentheses. [c] Sum of the intensities of the two degenerate species.

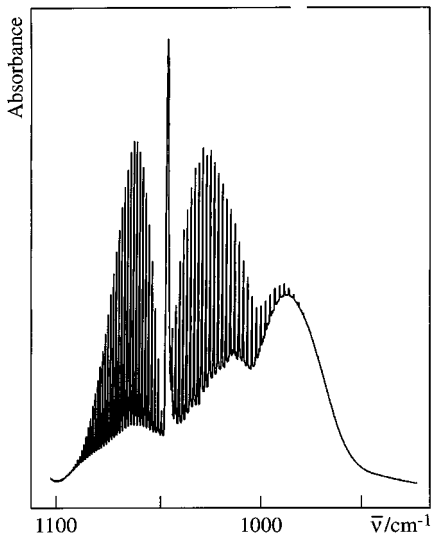

Figure 2. Vapor-phase infrared spectra of the CF stretch region, at 205 K, of a mixture of CH_3F and BF_3.

If a similar broadening is applied to the pure B type band by an extraconvolution with a Lorentzian slit of 4 cm^{-1}, the QQ splitting completely disappears, leaving a contour in which the P,Q,R structure is but barely visible. Thus, the absence of rotational structure in the 991 cm^{-1} band is not inconsistent with a B type contour. The substantial broadening necessary to rationalize the experimental contour most likely is due to

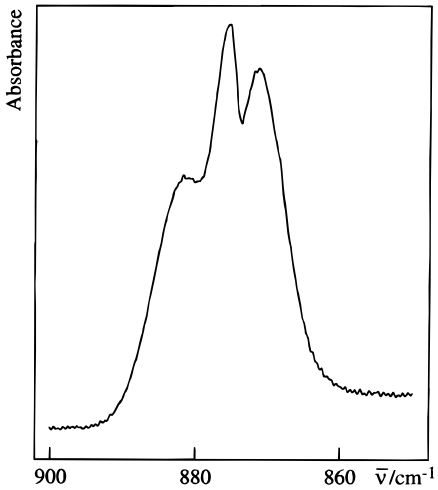

Figure 3. Vapor-phase infrared spectra in the BF_3 symmetric stretch region, at 205 K, of a mixture of CH_3F and BF_3.

pronounced anharmonic influences. This must be the consequence of the weakness of the van der Waals bond and the nonrigidity of the complex.

A similar complex band with nondescript contour was observed for the first overtone of the CF stretch. Candidates for producing complex bands are the CH stretches. However, the complex rotational structure of the gas-phase spectrum of CH_3F in this region obscured possible complex bands.

More interesting is the band at 875.6 cm^{-1} shown in Figure 3. This band is only present in spectra of mixtures of CH_3F and BF_3 and occurs quite far from infrared absorption bands in either CH_3F or BF_3. Its frequency, however, is close to the ν_1 vibration of BF_3, which is known[10] from vapor-phase Raman measurements to occur at 888 cm^{-1}. Although this band is infrared-forbidden in monomer BF_3, the ab initio calculations show that this transition in the complex has an intensity of 8 km mol^{-1}, a value of the same order of magnitude as, for instance, the high-frequency CH stretch modes. Therefore, we assign this band to the symmetric BF_3 stretch of the complex, ν_8. For the slightly nonplanar BF_3 moiety in the complex (vide infra), the symmetric stretch must have its dipole gradient very nearly parallel to the van der Waals bond. The latter is almost parallel to the *a* axis of the principal axis system, from which the bond dipole model predicts this mode to have predominantly type A contour. This is the contour shown by the 875.6 cm^{-1} band. The R branch of the band is substantially less intense than the P branch. As there are no other bands of the complex in the vicinity, it is unlikely that this intensity difference is caused by a coriolis interaction. The difference more probably is due to significant anharmonicity, reflecting, as for the 989 cm^{-1} band, the characteristics of the complex. The type A band calculated at 205 K shows a PR separation of 11.6 cm^{-1}. For the experimental band the maximum of the R branch is not well-defined, but the PR separation can be easily estimated to be near 11 cm^{-1}. In view of the anharmonic deformation of the band, this value is in sufficient agreement with the predicted value to support the assignment of the band as the symmetric BF_3 stretch of the complex.

The excess of BF_3 used in this experiment, together with the strength of the allowed BF_3 fundamentals, prevented other complex bands localized in the BF_3 moiety to be observed.

A decrease in temperature favors the formation of the complex. However, at lower temperatures the bands due to CH_3F and $CH_3F{\cdot}BF_3$ sharply decrease in intensity. This is attributed to partial condensation of the complex on the cell walls, due to the lesser volatility of the complex. The strong

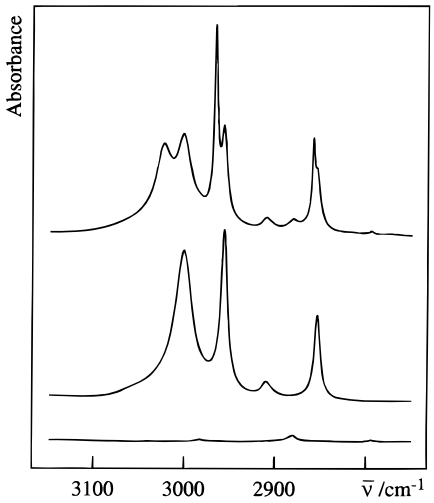

Figure 4. The CH stretch region of solutions in liquid krypton, at 128 K. Lower spectrum, solution of BF_3; middle spectrum, solution of CH_3F; top spectrum, solution of a mixture of CH_3F and BF_3.

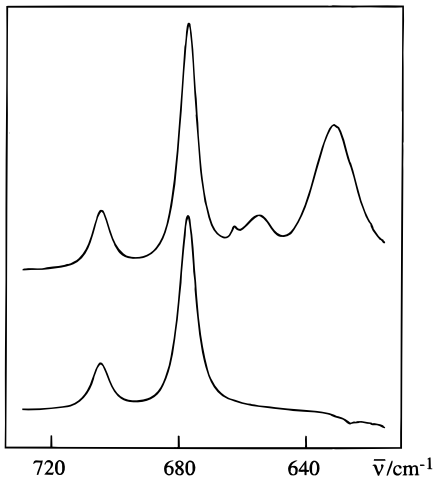

Figure 5. The $\nu_2(BF_3)$ region of solutions in liquid krypton, at 128 K. Lower spectrum, solution of BF_3; top spectrum, solution of a mixture of CH_3F and BF_3.

overlap of the bands in Figure 2 and the problems with the vapor pressure of the complex prevented data on the vapor-phase stability of the complex to be obtained.

3.3. Spectra in Liquid Krypton and Liquid Argon. The spectra in cryosolution of the monomers are well-known[11−13] and will not be discussed here. The behavior of mixtures of CH_3F and BF_3 in cryogenic solutions is exemplified by the spectra in Figures 4 and 5, which were recorded from solutions in liquid krypton (LKr). The frequencies observed for the complex $CH_3F{\cdot}BF_3$ are collected in Table 2. For the fundamental transitions, the experimental and ab initio complexation shifts, defined as ν(complex) − ν(monomer), are also given in this table.

The top trace in Figure 4 is the spectrum recorded at 127 K from a mixture, while the other spectra in this figure were recorded from solutions containing either CH_3F (middle trace) or BF_3 (lower trace). It is clear that the spectrum of the mixed solution is dominated by new bands, which must be due to the complex $CH_3F{\cdot}BF_3$. The complex bands appear blue-shifted from the monomer CH_3F bands. The shift is 23 cm^{-1} for the e mode, in excellent agreement with the 26.3 cm^{-1} predicted by ab initio for both $^{11}BF_3$ and $^{10}BF_3$. The bands at 2957 and 2859 cm^{-1} of CH_3F are an a_1 Fermi doublet. Both components blue shift upon complexation, although it can be seen that the shift of the high-frequency component is larger than that of the

TABLE 2: Experimental Frequencies and Complexation Shifts for $CH_3F \cdot BF_3$ in Liquid Krypton at 127 K[a]

assign.[b]	^{10}B ^{11}B	$\Delta\nu_{calc}(^{10}B/^{11}B)$	$\Delta\nu_{exp}(^{10}B/^{11}B)$
ν_1	3024	+26.3/+26.3	+23
ν_{14}	3024	+24.7/+24.7	+23
ν_2	2966	+15.9/+15.9	+9
$2\nu_4$	2859		
$\nu_8 + \nu_5$	2351 2301		
$\nu_8 + \nu_{16}$	2290		
$2\nu_8 + \nu_{10}$	2212		
$2\nu_7$	1992		
$\nu_5 + \nu_{10}$	1955 1907		
$\nu_{10} + \nu_{16}$	1896		
$\nu_8 + \nu_{10}$	1819		
ν_5	1485 1432	−8.1/−7.1	−8/−10
ν_{16}	1472 1419	−37.5/−36.2	−21/−23
$\nu_8 + \nu_{10}$	1346		
ν_7	1004	−34.6/−35.0	−31
ν_8	873	−13.7/−13.9	
ν_9	655 631	−71.9/−67.2	−50/−46
ν_{11}	159		
ν_{12}	104		

[a] All data in cm^{-1}. [b] Numbering of fundamentals as in Table 1.

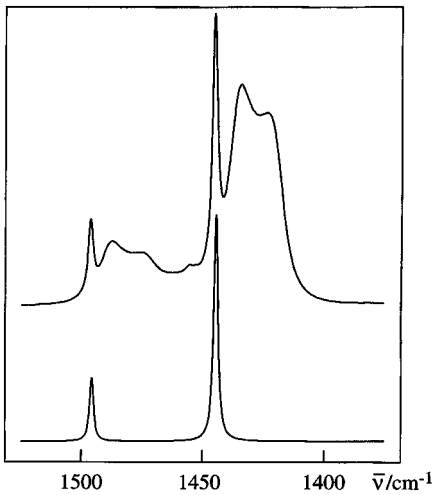

Figure 6. The $\nu_3(BF_3)$ region of solutions in liquid argon, at 95 K. Lower spectrum, solution of BF_3; top spectrum, solution of a mixture of CH_3F and BF_3.

low-frequency component. This shows that the Fermi resonance is somewhat changed by the complexation. Therefore, it is no surprise that the shift observed experimentally, 9 cm^{-1} for the more intense high-frequency component, agrees less well with the shift predicted by ab initio for the a_1 mode, 15.9 cm^{-1}.

Figure 5 gives the region of ν_2 of BF_3. It is clear that in the mixture new bands are observed on the low-frequency side of the ν_2 isotopic doublet. The shifts are −50 cm^{-1} for $\nu_2(^{10}BF_3)$ and −46 cm^{-1} for $\nu_2(^{11}BF_3)$, in reasonable agreement with the predicted shifts, −71.9 and −67.2 cm^{-1}, respectively.

In Figure 6, the region of $\nu_3(BF_3)$ is shown. For both isotopes, red-shifted new bands occur for the mixture. The ν_3 mode is degenerate in monomer BF_3. In agreement with this, the monomer bands are sharp singlets. However, in the complex for both isotopes a doublet is observed. This demonstrates that in the complex the 3-fold symmetry of the monomer has been removed, as was predicted by the ab initio calculations. The splittings of these modes are in agreement with the predicted ab initio frequencies: the calculated shifts for $\nu_2(^{10}B)$ are −8.1 and −37.5 cm^{-1}, while the observed shifts are −8 and −21 cm^{-1}, respectively, with similar results for $\nu_2(^{11}B)$. Another remarkable characteristic of these complex bands is their much increased width, compared with the monomer modes. A broadening, although less pronounced, can also be seen for the

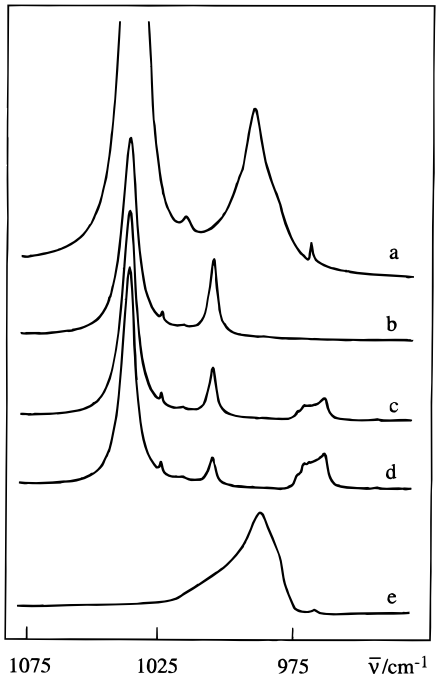

Figure 7. The CF stretch region of CH_3F. Spectrum a, supersaturated solution of CH_3F in liquid argon at 85 K; spectra b−d, solution of a mixture of CH_3F and BF_3in liquid argon at 104.7 K (b), at 102.5 K (c), and at 99.8 K (d); spectrum e, solid CH_3F at 10 K.

complex bands in Figure 5, which are also due to modes localized in the BF_3 moiety. This broadening, just as for the vapor phase spectra, is evidence supporting the nonrigidity of the complex predicted by the calculations.

Just as for the gas phase, in cryogenic solution a complex band is also observed, at 873 cm^{-1}, which must be assigned as the symmetric BF_3 stretch.

The complexation was also investigated in liquid argon (LAr). At the highest temperatures in this solvent, near 110 K, complex bands are observed that are extremely similar to those in liquid krypton, with frequencies in liquid argon typically 2−3 cm^{-1} higher. At lower temperatures, new bands start to emerge, as is illustrated in Figure 7. The top spectrum in this figure was recorded at 85 K from a highly concentrated solution of CH_3F. Comparison with the solid-state spectrum of CH_3F, recorded at 10 K, Figure 7e, shows that the band centered at 990 cm^{-1} is due to solid CH_3F suspended in the solution. Parts b−d of Figure 7 are recorded from mixed BF_3/CH_3F solutions. Obviously, the band at 1006 cm^{-1} is due to the dissolved complex. In the spectra recorded at 102.5 K (7c) and at 99.8 K (7d), new bands occur near 960 cm^{-1}. We assign these bands to solid $CH_3F \cdot BF_3$ crystallized from the saturated solution. This solid more than probably corresponds to the solid compound obtained by Oláh et al.[2] by treating methyl fluoride with boron trifluoride at low temperatures.

Figure 8 shows the far-infrared spectra of a concentrated mixture of BF_3 and CH_3F in LKr, at 134 and at 114 K. The two bands in the high-temperature spectrum, at 159 and at 104 cm^{-1} must be assiged to the complex, as the monomers show no bands in this region. It is clear from Table 1 that the ab initio calculations predict that only three of the six van der Waals modes will show appreciable infrared intensity. The lowest of these, calculated at 32.6 cm^{-1}, falls outside the spectral region studied, and therefore, the observed bands must be correlated with the transitions calculated at 187.4 and 122.7 cm^{-1}. Not only are the observed frequencies close to the predicted ones but the experimental relative intensity also agrees well with prediction. In terms of internal coordinates, all van der Waals

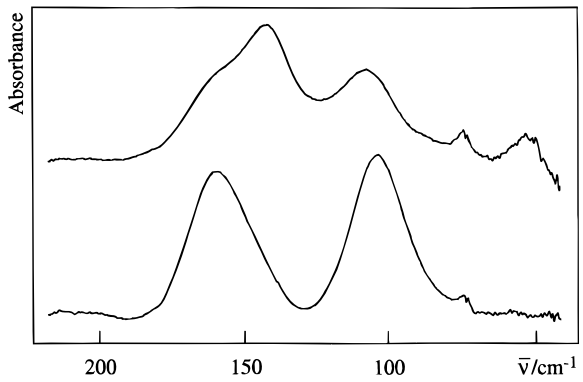

Figure 8. Far-infrared spectra of a solution of CH_3F and BF_3 in liquid krypton. The lower spectrum was recorded at 134.3 K, the top spectrum at 124.5 K.

modes are severely coupled. However, close analysis of the vibrations shows that the 159 cm^{-1} band is mainly a bending mode, while the 104 cm^{-1} mode is dominated by the stretching of the van der Waals bond.

At the lowest temperatures, as is clear from Figure 8, new bands are found in the spectra. As the latter were recorded from concentrated solutions, these new bands are assigned to the same crystalline complex which was also observed in the mid-infrared spectra of the LAr solutions.

3.4. Stoichiometry of the Complex. The stoichiometry of the complex was checked in the usual way[14] from a series of solutions in LKr in which the concentrations of the monomers were systematically varied. The analysis requires integrated intensities for each of the species involved. For the complex and CH_3F the C−H stretching region between 3150 and 2775 cm^{-1} was used. From the experimental spectrum of a mixture, a rescaled spectrum of CH_3F was subtracted in such a way that the contributions due to the complex were isolated. The rescaled CH_3F spectrum and the complex contributions were then numerically integrated to yield I_{CH_3F} and $I_{CH_3F\cdot BF_3}$. For the intensities of BF_3 a similar procedure was followed in the region between 2385 and 2300 cm^{-1}, now by rescaling a spectrum of BF_3 to optimally reproduce the BF_3 contributions to the experimental spectrum and subsequently integrating the rescaled spectrum to yield I_{BF_3}. The intensities $I_{CH_3F\cdot BF_3}$ were then plotted against $I_{BF_3} \times I_{CH_3F}$, $I_{BF_3} \times (I_{CH_3F})^2$, and $(I_{BF_3})^2 \times (I_{CH_3F})$. Only in the first case was a linear plot obtained, confirming the 1:1 stoichiometry of the complex.

3.5. Complexation Enthalpy. The complexation enthalpy $\Delta H°$ for the complex was calculated from the slope of the linear regression of the van't Hoff graphs[15] in which the intensity ratio $I_{CH_3F\cdot BF_3}/(I_{BF_3} \times I_{CH_3F})$ was plotted versus $1/T$. This analysis was made for solutions in LKr and in LAr. For the solutions in LKr, intensities were obtained by numerical integration of the band at 3322 cm^{-1}; for monomer BF_3, the band at 2050 cm^{-1}; for monomer CH_3F, and the symmetric BF_3 stretch at 873 cm^{-1} for the complex. The temperature interval ranged from 116 to 164 K, with the midpoint of the van't Hoff plot corresponding to a temperature of 140 K. For the solutions in LAr, numerically integrated intensities of the bands at 706 and 681 cm^{-1} were summed and used for monomer BF_3, while the intensities for monomer CH_3F and for the complex were taken from a least squares band fitting, using Gauss/Lorentz sum functions, of the 1080−970 cm^{-1} CF stretch region. The solubility problems with the complex, discussed above, limited the temperature interval from 105 to 116 K, with the midpoint of the van't Hoff plot corresponding to 110 K. The van't Hoff plots are shown in Figure 9. The slope of the linear regression, corrected for thermal expansion of the solutions[15] yielded a $\Delta H°$

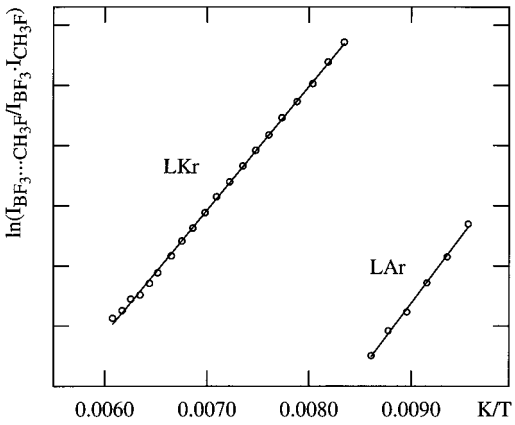

Figure 9. van't Hoff plots for the 1:1 complex between CH_3F and BF_3 in liquid krypton (LKr) and in liquid argon (LAr).

of −18.0(3) kJ mol^{-1} for the solution in LKr and −16.8(5) kJ mol^{-1} for the solution in LAr. The statistical uncertainties on these results are very small, reflecting the high degree of linearity of the van't Hoff plots. However, the $\Delta H°$ for LAr should be treated with some caution, as the study covers a very limited temperature interval only.

4. Discussion

The dipole moment of BF_3 is zero, and the MP2/6-31G** dipole moments of CH_3F and of the complex are 2.161 and 2.838 D, respectively. The increase in dipole moment upon complexation can be ascribed to two phenomena. First, in the complex the BF_3 moiety is no longer planar, resulting in a dipole moment along the BF_3 axis. Second, the dipoles and higher multipoles of the constituent molecules will induce a dipole moment in the opposing moiety.

The magnitude of the first contribution can be estimated by calculating the dipole moments of the constituent molecules at the same level as that of the complex using the geometry they have in the complex. This results in a moment of 2.231 D for CH_3F and 0.350 D for BF_3. The former hardly differs from that of the isolated monomer, showing that the geometry of this molecule is not greatly affected by the complexation. The value obtained for BF_3 can be rationalized as follows. For monomer BF_3, the charges on the fluorine atoms have been estimated to be near 0.5 electron.[16] This value, together with the average ab initio BF bond length leads to a bond dipole moment for a B−F bond of 3.200 D. The B−F bonds show an angle of 87.448° with the BF_3 axis, and the three bond moments result in a dipole moment of 0.427 D for the BF_3 moiety. Considering the approximations made to reach this value, it compares favorably with the ab initio value of 0.350 D. The BF_3 axis is nearly parallel to the van der Waals bond, so that the BF_3 dipole moment also is nearly parallel to this bond. The CH_3F molecule is but slightly deformed in the complex, and consequently, its dipole moment lies nearly parallel to the C−F bond. The subtraction of the vector sum of the moments of the CH_3F and BF_3 moieties from that of the complex results in a difference vector also nearly parallel to the van der Waals bond, with a length of 0.664 D. This difference vector is the induced dipole moment. Concludingly, it is clear that both the nonplanarity of the BF_3 moiety and the induced effects contribute, with similar magnitude, to the increased dipole moment of the complex.

Using the formula of Pross et al.,[17] it is easily shown that the BF_3 grouping shows a negative tilt angle of −0.640°, i.e., the symmetry axis of BF_3 is rotated away from the van der Waals bond, in the symmetry plane of the complex, in such a

TABLE 3: Solvation Energies and Solvent Contribution to the Complexation Enthalpy[a]

	LAr	LKr
BF_3	−3.715	−4.637
CH_3F	−3.002	−3.676
$CH_3F{\cdot}BF_3$	−4.533	−5.565
ΔH^{solv}	2.184	2.748

[a] All data in kJ mol^{-1}.

way that the in-plane B−F bond is tilted away from the (C)F atom. Similarly, for the methyl group a positive tilt angle of 0.333° is calculated. The negative tilt of the BF_3 moiety can be rationalized in terms of the interaction of the out-of-plane fluorine atoms with the out-of-plane hydrogen atoms. The distance between a hydrogen and the fluorine atom on the same side of the symmetry plane is 2.95 Å. This is slightly larger than the sum of the van der Waals radii of these atoms, 2.30 Å. Therefore, the interaction must be attractive, leading to the negative tilt of the BF_3 moiety. However, for the same reason the tilt of the methyl group should be negative, while a small positive value is calculated. A possible explanation for this effect is that a small negative tilt of the methyl group is off-set by a larger positive tilt which occurs as a consequence of the same hyperconjugative interaction that causes the positive tilt in, for instance, the staggered conformer of methanol.[17]

The uncorrected complexation energy calculated in this study, −25.97 kJ mol^{-1}, is larger than the value calculated[2] using a sophisticated basis set for $HF{\cdot}BF_3$, −16.3 kJ mol^{-1}. Apart from differences due to the different basis sets, the higher stability of $CH_3F{\cdot}BF_3$ is in line with qualitative expectations, as the methyl group acts as an electron donor compared to hydrogen, and which is in agreement with the shorter van der Waals bond length in $CH_3F{\cdot}BF_3$, 2.42 Å,[6] than that in $HF{\cdot}BF_3$, 2.544(2) Å.[3] Evidently, the calculated complexation energy cannot be directly compared with the complexation enthalpies determined in the cryosolutions. Therefore, the latter were transformed into gas-phase $\Delta H°$s by correcting for solvent influences, and subsequently statistical thermodynamical corrections were applied to extract the zero-point energy difference.

The solvent contribution to the complexation enthalpy, ΔH^{solv}, is defined as the difference between the complexation enthalpies in solution and gas phase:

$$\Delta H^{solv} = \Delta H°(sol) - \Delta H°(gas)$$

This quantity can be expressed in terms of the solvation enthalpies of the individual species as

$$\Delta H^{solv} = H^{solv}(CH_3F{\cdot}BF_3) - H^{solv}(CH_3F) - H^{solv}(BF_3)$$

Solvation energies for the individual species, defined as the difference in energy of the molecule in solution with that of the isolated molecule, were calculated by ab initio methods, using the self-consistent isodensity polarizable continuum model[18] at the RHF/6-311+G** level. These energies were calculated for solutions in LAr (relative permittivity $\kappa = 1.52$) and in LKr ($\kappa = 1.69$), and the results are collected in Table 3. All energies can be seen to be negative, i.e., all species are stabilized by the solvents. In agreement with the higher polarizability of krypton, the solvent stabilizations in LKr are higher than in LAr. It may be remarked that the solvation energy for BF_3, for which the dipole moment is zero, is very high, which is due to the high charges on the atoms of this molecule, discussed above. For the present purpose, we identify the solvation energies with solvation enthalpies $H^{solv}(i)$, so that using the data of Table 3, the ΔH^{solv} can be calculated. The resultant values are also given in Table 3. For both solvents, ΔH^{solv} is positive, i.e., the complexation enthalpy in the gas phase will be higher than that in solution. The larger effect in LKr of course is related to the higher polarizability of krypton. The gas-phase enthalpies $\Delta H°$(gas) calculated using the ΔH^{solv} are −20.7(3) and −19.0(5) kJ mol^{-1} starting from the solution values for LKr and LAr, respectively. Next, the zero-point vibrational, the thermal, and the pV contributions to the enthalpy of each species were calculated using straightforward statistical thermodynamics. The translational and rotational contributions were obtained in the classical limit, and isotopically averaged vibrational contributions were calculated in the harmonic approximation using the uncorrected ab initio vibrational frequencies. For use with the enthalpy derived from the LKr solutions, these calculations were performed at 140 K, while for use with the LAr value, the calculations were made at 110 K, i.e., at the respective midpoints of the van't Hoff plots used to obtain the $\Delta H°$ in solution. The statistical thermodynamical quantities were then used to calculate the zero-point energy differences from the $\Delta H°$(gas). This leads to a complexation energy of −23.4(3) kJ mol^{-1} when starting from the LKr data and of −21.3(5) kJ mol^{-1} using the LAr data. The uncertainties quoted are those on the experimental values of $\Delta H°$, and, in view of the nature of the corrections, presumably are overoptimistic. As solvent and thermal influences have been removed, these two results should be identical; however, they differ by about 10%. This, in part, can be ascribed to the approximate way in which the solvent and thermal corrections were calculated. However, by all qualitative arguments the solvent and thermal contributions for the LAr solutions must be smaller than those for LKr, in agreement with the above calculations. Hence, starting from the same zero-point energy difference, the complexation enthalpy in LAr should be higher than that in LKr, opposite to the experimental results reported above. It is believed that this discrepancy is due to the less reliable value for the $\Delta H°$ in LAr, which, as was stressed above, was determined in a very limited temperature interval.

The more reliable result, i.e., the one obtained for LKr, leads to a complexation energy, −23.4(3) kJ mol^{-1}, which is significantly larger than the solution enthalpy and which is in good agreement with the MP2/6-31+G** complexation energy of −25.97 kJ mol^{-1}.

5. Conclusion

In this study we have investigated, using infrared spectroscopy, mixtures of CH_3F and BF_3 at low temperatures in the gas phase and in liquid krypton and argon. In all cases, the formation of a 1:1 complex was observed. The complexation enthalpy was determined to be −18.0(3) kJ mol^{-1} in liquid krypton and −16.8(5) kJ mol^{-1} in liquid argon. The spectra show that in the complex the 3-fold symmetry axis of BF_3 is lost. Ab initio calculations at the MP2/6-31G** level confirm the formation of a complex with C_s symmetry. The complex has a van der Waals bond between the boron atom and the fluorine atom of methyl fluoride, and the C−F bond makes an angle of 118° with the van der Waals bond. The experimental complexation enthalpy for solutions in liquid krypton is consistent with the ab initio complexation energy.

Acknowledgment. The FWO (Belgium) is thanked for a grant toward the spectroscopic equipment used in this study. W. Herrebout and G. Everaert are thanked for help with the ab initio calculations. Financial support by the Flemish Community, through the Special Research Fund (BOF), is gratefully acknowledged.

References and Notes

(1) March, J. *Advanced Organic Chemistry*, 4th ed.; Wiley-Interscience: New York, 1992; p 535.

(2) Oláh, G.; Kuhn, S.; Oláh, J. *J. Chem Soc.* **1957**, 2174.

(3) Phillips, J. A.; Canagaratna, M.; Goodfriend, H.; Grushow, A.; Almlöf, J.; Leopold, K. R. *J. Am. Chem. Soc*. **1995**, *117*, 12549.

(4) Bertrán, J.; Mora, F.; Silla, E. *J. Chem. Soc., Perkin Trans. 2* **1982**, 647.

(5) Arnau, A.; Bertrán, J.; Silla, E. *J. Chem. Soc., Perkin Trans. 2* **1989**, 509.

(6) Leopold, K. R.; Canagaratna, M.; Philips, J. A. *Acc. Chem. Res*. **1997**, *30*, 57.

(7) Herrebout, W. A.; Van der Veken, B. J. *J. Phys. Chem*. **1993**, *97*, 10622.

(8) Frisch, M. J.; Trucks, G. W.; Schlegel, H. B.; Gill, P. M. W.; Johnson, B. G.; Robb, M. A.; Cheeseman, J. R.; Keith, T.; Petersson, G. A.; Montgomery, J. A.; Raghavachari, K.; Al-Laham, M. A.; Zakrzewski, V. G.; Ortiz, J. V.; Foresman, J. B.; Cioslowski, J.; Stefanov, B. B.; Nanayakkara, A.; Challacombe, M.; Peng, C. Y.; Ayala, P. Y.; Chen, W.; Wong, M. W.; Andres, J. L.; Replogle, E. S.; Gomperts, R.; Martin, R. L.; Fox, D. J.; Binkley, J. S.; Defrees, D. J.; Baker, J.; Stewart, J. P.; Head-Gordon, M.; Gonzalez, C.; Pople, J. A. *Gaussian 94*, Revision B.2; Gaussian, Inc.: Pittsburgh, PA, 1995.

(9) Van der Veken, B. J. In *Computing Applications in Molecular Spectroscopy*; George, W. O., Steele D., Eds.; The Royal Society of Chemistry: Cambridge, 1995; p 105.

(10) Nakamoto, K. *Infrared and Raman Spectra of Inorganic and Coordination Compounds*, 4th ed.; J. Wiley and Sons: New York, 1986; p 123.

(11) Sluyts, E. J.; Van der Veken, B. J. *J. Am. Chem. Soc*. **1996**, *118*, 440.

(12) Kolomiitsova, T. D.; Mielke, Z.; Tokhadze, K. G.; Shchepkin, D. N. *Opt. Spectrosc. (USSR)* **1979**, *46*, 391.

(13) Barri, M. F.; Tokhadze, K. G. *Opt. Spectrosc. (USSR)* **1981**, *51*, 70.

(14) Herrebout, W. A.; Van der Veken, B. J. *J. Phys. Chem*. **1996**, *100*, 15695.

(15) Van der Veken, B. J. *J. Phys. Chem*. **1996**, *100*, 17436.

(16) Fowler, P. W.; Stone, A. J. *J. Phys. Chem*. **1987**, *91*, 509.

(17) Pross, A.; Radom, L.; Riggs, N. V. *J. Am. Chem. Soc*. **1980**, *102*, 2253.

(18) Foresman, J. B.; Keith, T. A.; Wiberg, K. B.; Snoonian, J.; Frish, M. J. *J. Phys. Chem*. **1996**, *100*, 16098.